# One- and two-dimensional rare earth–copper molecular materials

Olivier Guillou, Olivier Kahn*, Robert L. Oushoorn
*Laboratoire de Chimie Inorganique, URA CNRS no. 420, 91405 Orsay (France)*

Kamal Boubekeur and Patrick Batail*
*Laboratoire de Physique du Solide, URA CNRS no. 002, Université de Paris-Sud, 91405 Orsay (France)*

**Abstract**

This short review paper deals with the crystal structures and the magnetic properties of molecular materials arising from the reaction of the $[Cu(pba)]^{2-}$ precursor with trivalent rare earth ions M(III); pba stands for 1,3-propylenebis(oxamato). Three families of compounds have been obtained so far, abbreviated as $M_2Cu_3Cu \cdot \mathbf{1}$, $M_2Cu_3 \cdot \mathbf{2}$ and $M_2Cu_3 \cdot \mathbf{3}$, depending on the synthesis method, and/or the nature of the rare earth. The structure **3** is the simplest one; it consists of discrete and infinite ladder-motifs, the edges of which are made of MCu(pba) units (M going from Tb to Yb, and Y), and the rungs of Cu(pba) units linking two rare earth ions. In structure **1** (M going from La to Gd), the ladders are linked together by oxalato groups, promoting a double-sheet two-dimensional pattern. In addition, this structure contains discrete $[Cu(H_2O)_5]^{2+}$ cations interspersed in the gap between the layers. Finally, structure **2** (M going again from La to Gd) consists of discrete and infinite tube-like motifs with a pseudo four-fold symmetry, resulting from the condensation of two ladder-motifs associated with a complete rearrangement of the rungs. The temperature dependences of the magnetic susceptibility and the field dependences of the magnetization for all compounds have been investigated. Only some of the findings are discussed. For the compounds with M = Gd, Tb, Dy and Er, $\chi_M T$ ($\chi_M$ being the molar magnetic susceptibility, and $T$ the temperature) increases as $T$ is lowered. This result together with the magnetization data indicate that the M(III)–Cu(II) interaction is ferromagnetic. When M = La, the copper(II) spin carriers are weakly antiferromagnetically coupled through the diamagnetic rare earth ion. The same situation holds for M = Eu which has also a diamagnetic ground state. On the other hand, there is no propagation of the interaction through the Y(III) ion. The perspectives in this new field of the molecular materials incorporating rare earth and 3d metal ions are briefly discussed.

## Introduction

Since two decades or so, a large number of heterobimetallic molecular species have been described [1]. Particular emphasis has been placed on the magnetic properties of these compounds. Indeed, the interaction between two non-equivalent magnetic centers may lead to situations which cannot be encountered with species containing only one kind of spin carrier. One of the most remarkable results along this line is the strict orthogonality of the magnetic orbitals realized in Cu(II)VO(II) [2], Cu(II)Cr(III) [3] or Ni(II)Cr(III) [4] species. Another interesting result is the parallel alignment of high local spins owing to the presence of small local spins between them as schematized:

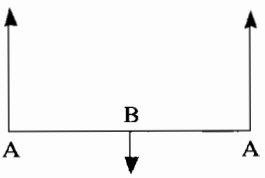


This happens, for instance, in an Mn(II)Cu(II)Mn(II) species with an $S = 9/2$ ground state spin [5], or in an Mn(II)–nitronyl nitroxide ring hexamer with an $S = 12$ ground state spin which might well be so far the molecular compound with the highest spin in the ground state [6].

More recently, the first heterobimetallic chain compounds have been synthesized and studied [7–18]. If the interaction between nearest neighbor magnetic centers is antiferromagnetic, those chains exhibit the one-dimensional ferrimagnetic behavior characterized by a minimum in the $\chi_M T$ versus $T$ plot, $\chi_M$ being the molar magnetic susceptibility per repeat unit and $T$ the temperature. In the low-temperature range, a ferrimagnetic

*Authors to whom correspondence should be addressed.

0020-1693/92/$5.00

chain with $S_A$ and $S_B$ local spins qualitatively behaves as a ferromagnetic chain of $|S_A - S_B|$ spins as shown:

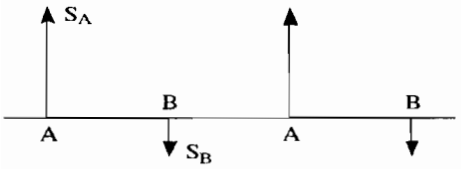


The most striking finding concerning the ferrimagnetic chains is the design of molecular-based magnets exhibiting a spontaneous magnetization below a critical temperature $T_c$ [10–12, 17, 18]. These molecular-based magnets are constructed by assembling ferrimagnetic chains in the crystal lattice in a ferromagnetic fashion. The highest $T_c$ reported so far for compounds of this kind is apparently 30 K.

Let us turn back for a moment to heterobimetallic molecular species. Gatteschi and co-workers reported on Cu(II)Gd(III)Cu(II) trinuclear species with Gd(III)–$O_2$–Cu(II) ferromagnetic interactions so that the ground state spin was $S = 9/2$ [19, 20]. Subsequently they proposed a mechanism accounting for this unexpected result; the copper(II) unpaired electron is partially delocalized toward the empty 6s rare earth orbital, which favors the parallel alignment with seven 4f electrons based on Hund's rule [21]. The ferromagnetic nature of the Gd(III)–Cu(II) pair has been recently confirmed by Matsumoto *et al.* [22].

This sequence of findings concerning heterobimetallic chain compounds with 3d transition ions, and heterobimetallic molecular species with both 3d and rare earth ions prompted us to launch a new project dealing with low-dimensional systems incorporating both 3d and rare earth ions. In a first step, we have explored the reaction of the copper(II) precursor $[Cu(pba)]^{2-}$ schematized below:

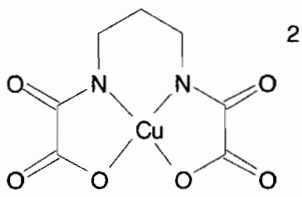


where pba stands for 1,3-propylenebis(oxamato) with trivalent rare earths. This short review will sum up the main findings obtained so far, and will report on a new family of compounds in the system $[Cu(pba)]^{2-}$/rare earth(III).

## Three families of compounds

The dianionic copper(II) precursor $[Cu(pba)]^{2-}$ reacts with divalent transition metal ions M(II) in a solvent S to afford one-dimensional compounds of formula $MCu(pba)\cdot nS$ [9, 10]. If $[Cu(pba)]^{2-}$ reacts with a trivalent metal ion M(III), one could expect to obtain compounds of higher dimensionality of formula $M_2[Cu(pba)]_3\cdot nS$. Before undertaking this work, we thought that a plausible structure when M is a rare earth would consist of infinite layers of hexagonal rings with a rare earth occupying each of the corners, and the edges made up of Cu(pba) units as schematized below where –Cu– stands for Cu(pba) bridging two rare earth atoms:

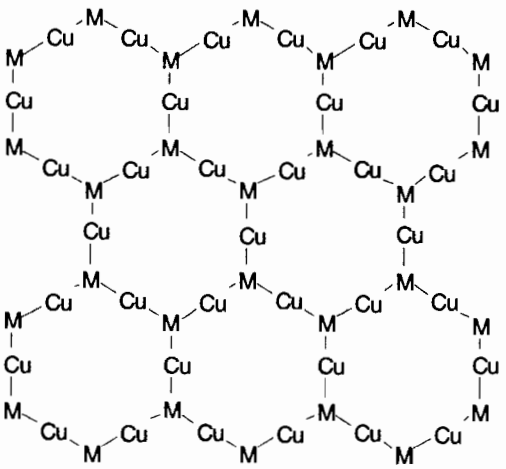


Such a structure is reminiscent of that of $M_2(ox)_3\cdot 9.5H_2O$ (M = La or Gd) with ox = oxalato replacing Cu(pba) [23, 24].

Actually, we have not found such a structure yet. Rather, we have obtained three families of compounds whose construction derives from a common structural principle, with specific differences according to the nature of the rare earth, and/or the synthesis method. Family **1** concerns the compounds of formula $M_2(ox)[Cu(pba)]_3[Cu(H_2O)_5]\cdot 20H_2O$ (hereafter abbreviated as $M_2Cu_3Cu\cdot$**1**) with M going from La to Gd. Pm which is radioactive has been ignored. Family **2** concerns compounds of formula $M_2[Cu(pba)]_3\cdot 23H_2O$ (hereafter abbreviated as $M_2Cu_3\cdot$**2**) with M going again from La to Gd. Finally, family **3** deals with compounds of formula $M_2[Cu(pba)]_3\cdot 23H_2O$ (hereafter abbreviated as $M_2Cu_3\cdot$**3**) with M going from Tb to Yb; M may be also Y. The details of the synthesis of the compounds will be given at the end of the paper. We must mention here, however, that the compounds of families **1** and **3** are prepared according to the same method, namely the slow diffusion of aqueous solutions of trivalent rare earth chloride and $Na_2[Cu(pba)]$. The nature of the obtained compound only depends on the nature, and hence the size of the rare earth. On the other hand, the compounds of family **2** are synthesized by a more exotic method. Altogether, twenty-one compounds have been characterized so far, as specified in Table 1.

To our knowledge, Galy and co-workers have been the only authors so far to describe extended molecular

TABLE 1. Rare earth(III)–copper(II) compounds prepared from the copper(II) precursor $[Cu(pba)]^{2-}$. The sign x indicates that the compound has been prepared and characterized; the sign x̲ indicates that it exhibits a ferromagnetic-like behavior, i.e. an increase of $\chi_M T$ as $T$ is lowered

| | La | Ce | Pr | Nd | Sm | Eu | Gd | Tb | Dy | Ho | Er | Tm | Yb | Y |
|---|---|---|---|---|---|---|---|---|---|---|---|---|---|---|
| $M_2Cu_3Cu \cdot 1$ | x | x | x | x | x | x | x̲ | | | | | | | |
| $M_2Cu_3 \cdot 2$ | x | x | x | x | x | x | x̲ | | | | | | | |
| $M_2Cu_3 \cdot 3$ | | | | | | | | x̲ | x̲ | x | x̲ | x | x | x |

lattices incorporating both rare earth and 3d metal ions. Beside pentanuclear $M_2Ni_3$ [25] and tetranuclear $M_2Ni_2$ [26] species, they also reported on MNi chain compounds with either dithiooxalato and oxalato [27, 28], or dithiooxalato and glycine [29] bridges. The crystal structures of most of those compounds are quite original, and often magnificient. On the other hand, in all compounds, the 3d metal ion is Ni(II) in $-S_4$ square planar surroundings, and therefore diamagnetic. It follows that the magnetic properties could only originate in the sum of the rare earth contributions, and no rare earth–rare earth interaction was detected. Other mixed rare earth–copper clusters of high nuclearity, up to eight metal ions, were recently reported [30–32]; the physical properties of those interesting species have not been investigated yet.

## Overview on the crystal structures

Some information on the crystal structures of compounds belonging to families **1** [33] and **2** [34] has already been given. On the other hand, structure **3** has not been reported yet.

We will begin by the description of this structure **3** which is actually the simplest one. This structure has been solved for M = Dy. It consists of discrete, infinite ladder-like motifs shown in Fig. 1. The asymmetric unit content along with the atom labelling is shown in Fig. 2. The edges of the ladder are made of MCu(pba) units with a strict alternation of rare earth and copper atoms bridged by oxamato groups. As for the rungs of the ladder, they are made of Cu(pba) units linking two rare earth atoms belonging to both edges of the ladder. When seen along the direction of a rung, the two edges of a ladder are in an eclipsed configuration. This is due to the wrinkled arrangement of the ladders, contrasting with the puckered arrangement of the same motif in structures **1** and **2** (see below). Each Dy atom is surrounded by eight oxygen atoms, six of them belonging to three Cu(pba) groups, the other two to water molecules. The Dy coordination polyhedron shown in Fig. 3(a) may be described as a distorted square antiprism. The copper atom adopts a square

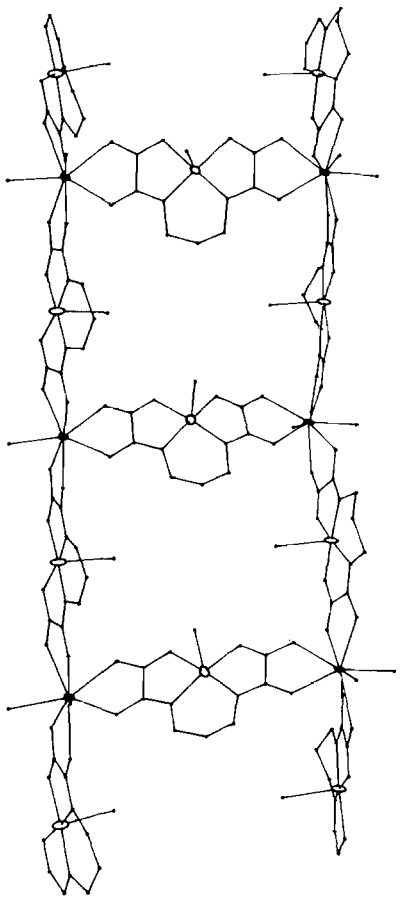

Fig. 1. Perspective view of the ladder-like motif in $Dy_2Cu_3 \cdot 3$. As in the other Figs., the rare earth atoms are noted in black, and the copper atoms in white.

pyramidal environment with two oxygen and two nitrogen atoms of the pba ligand in the basal plane, and a water molecule at the apex. The Dy–Cu separations across the oxamato bridge range from 5.6013(22) to 5.7143(23) Å, and the separation between two Dy atoms connected in the transverse direction is 11.3390(10) Å. Within the lattice, the ladders are parallel to each other, and organized in such a way that each ladder is surrounded by four identical ladders as depicted in Fig. 4. Such an organization creates channels perpendicular to the plane of the ladders. These channels are

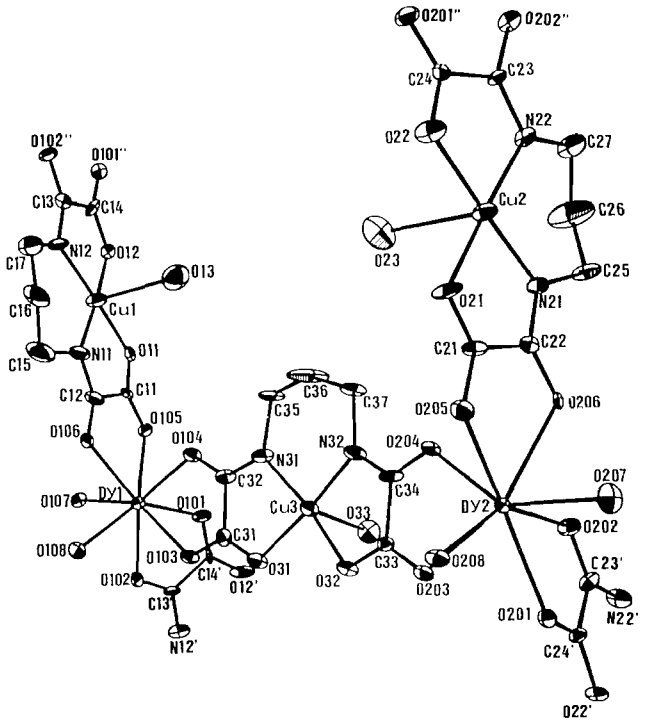


Fig. 2. Asymmetric unit content along with the atom labelling for $Dy_2Cu_3 \cdot 3$. Primed atoms have the symmetry $(\frac{1}{2}+x, \frac{1}{2}-y, \frac{1}{2}+z)$; double primed atoms have the symmetry $(x-\frac{1}{2}, \frac{1}{2}-y, z-\frac{1}{2})$.

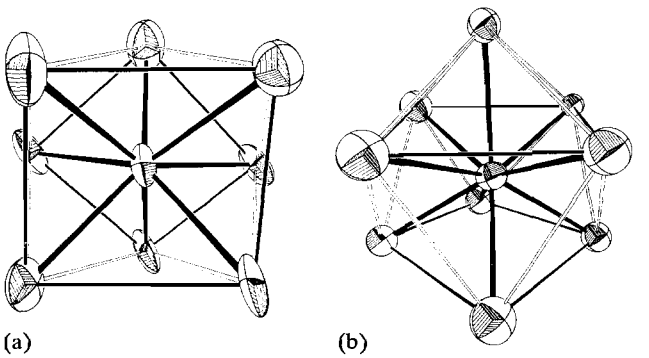

(a) (b)

Fig. 3. (a) Dysprosium coordination polyhedron in $Dy_2Cu_3 \cdot 3$. (b) Samarium coordination polyhedron in $Sm_2Cu_3 \cdot 2$. The black thin lines between oxygen atoms emphasize the staggered squares of the antiprism.

clearly apparent in Fig. 4. In addition to the seven water molecules coordinated to the metal ions in the $M_2[Cu(pba)]_3$ asymmetric unit, sixteen non-coordinated water molecules were located and refined, thus forming the basis of an intricate hydrogen bond network between the ladders.

The structure **1** has been solved for M = Gd. It can be constructed by the combination of ladder-type motifs rather similar to those described above, and oxalato bridges. When seen along the direction of a rung, the two edges of a ladder are staggered in structure **1**,

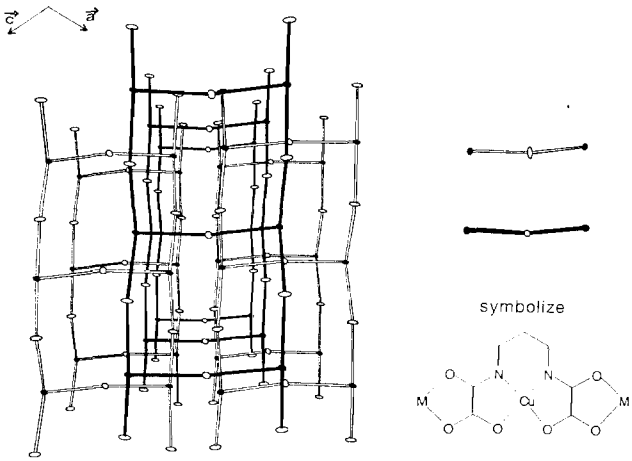


Fig. 4. Relative positions of the ladders in $Dy_2Cu_3 \cdot 3$. Note the channels in the direction perpendicular to the plane of the ladders.

instead of eclipsed in the wrinkled ladders of structure **3**. The ladders are no longer isolated from each other. Rather, they are associated across oxalato bridges along the *b* direction of the monoclinic lattice. These oxalato bridges promote a two-dimensional pattern of association of the ladders, with a double-sheet thick honeycomb network based on hexagonal rings as shown in Fig. 5. These rings have two opposite short edges Gd(ox)Gd with a Gd–Gd separation of 6.336(1) Å, and four long edges Gd[Cu(pba)]Gd with a mean Gd–Gd separation of 11.431 Å. The rare earth atom adopts a distorted capped square antiprism coordination of nine oxygen atoms, six of them provided by the Cu(pba) groups, two by the oxalato group, and the last one by a water molecule. The copper atom of the Cu(pba) unit retains the square pyramidal environment with a water molecule in the apical position. Altogether, the two-dimensional network of oxalato bridged ladders forms a dianionic frame formulated as $\{Gd_2(ox)[Cu(pba)]_3\}^{2-}$. Dications $[Cu(H_2O)_5]^{2+}$ are interspersed in the gap between the layers, anchoring the slabs to each other along the transverse *c* axis direction. Again, non-coordinated water molecules provide hydrogen bonds between the double layers.

The structure **2** was solved for M = Sm, and might well be the most remarkable. It can be seen as the condensation of two puckered ladders as found in structure **1** together with quite an unexpected redistribution of the rungs. These rungs undergo a collective, highly concerted criss-cross switching process to achieve an infinite tube-like motif of an essentially square section and quasi four-fold symmetry as schematized in Fig. 6. A schematic view down the pseudo four-fold symmetry axis *c* is shown in Fig. 7, and a stereoview of this remarkable structure in Fig. 8. The ladder rungs are

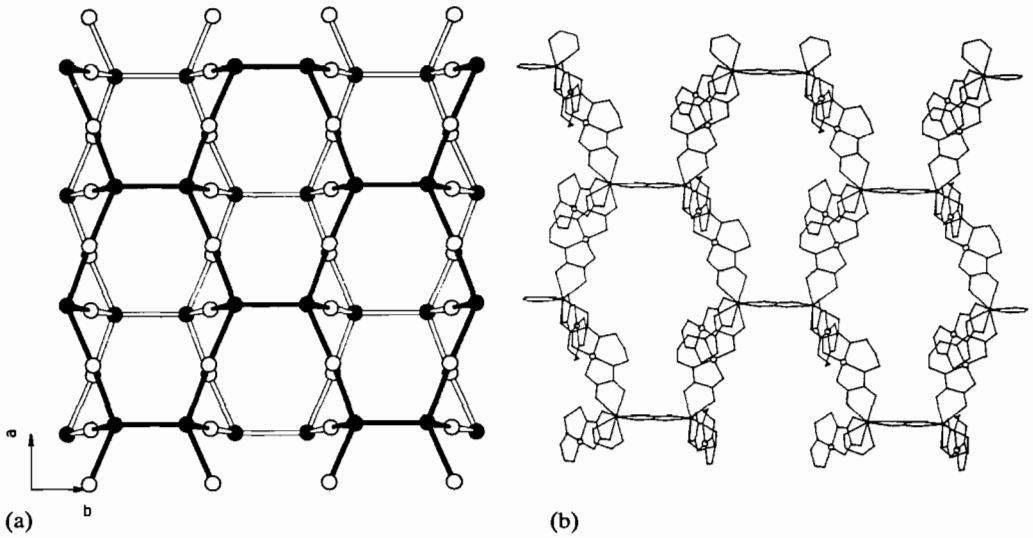


Fig. 5. (a) Schematic representation of four ladder-like motifs together by oxalato groups along the *b* direction for $Gd_2Cu_3Cu \cdot \mathbf{1}$. The solid (open) lines symbolize linkages within the upper (lower) layer. (b) Detail of the upper layer of the two-dimensional pattern. This Fig. emphasizes the honeycomb pattern of $Gd_6$ rings.

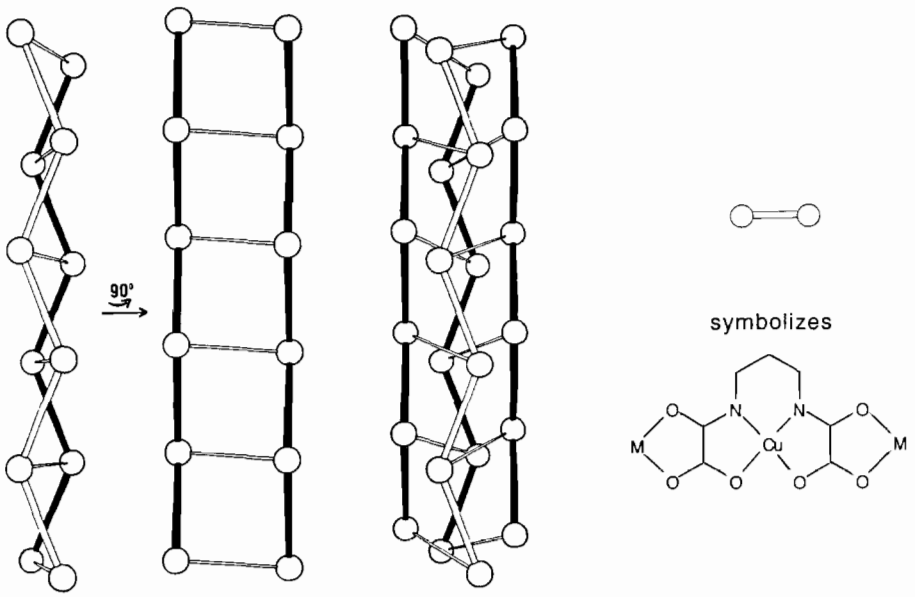


Fig. 6. Condensation of two ladder-like motifs as shown in Fig. 1 along with the redistribution of the ladder rungs to achieve the tube-like motif found in $Sm_2Cu_3 \cdot \mathbf{3}$.

intertwined by alternately switching from one edge of a ladder to that of the nearest orthogonal one. The intertwining of the ladder rungs creates an helicoidal pattern also exemplified in Figs. 7 and 8. As in structure **1**, the rare earth atom adopts a distorted capped square antiprism coordination of nine oxygen atoms as shown in Fig. 3(b). Six of the oxygen atoms come from three Cu(pba) groups, and three from water molecules. The copper coordination sphere is essentially unchanged as compared to **1** and **3**. The Sm–Cu separations through the oxamato group range from 5.675(7) to 5.762(7) Å, and the length of the ladder rungs is Sm–Sm = 11.357(5) Å.

## Magnetic properties

We do not intend here to discuss in detail the magnetic properties of all compounds. Several results are not fully understood yet. Some of them are quite surprising and will deserve a special investigation. Actually, we will focus on two aspects concerning the magnetism of those compounds.

### *Interaction between copper(II) ions through Y(III) and La(III) ions*

Two of the rare earths we have used are diamagnetic, namely Y(III) and La(III) (although strictly speaking

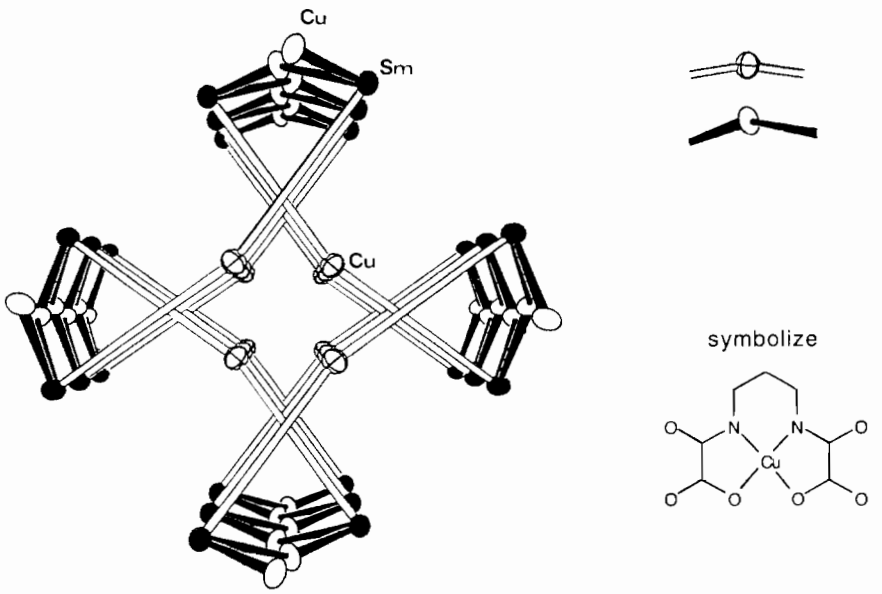


Fig. 7. Schematic representation of the tube-like motif with the pseudo four-fold symmetry in $Sm_2Cu_3 \cdot 2$.

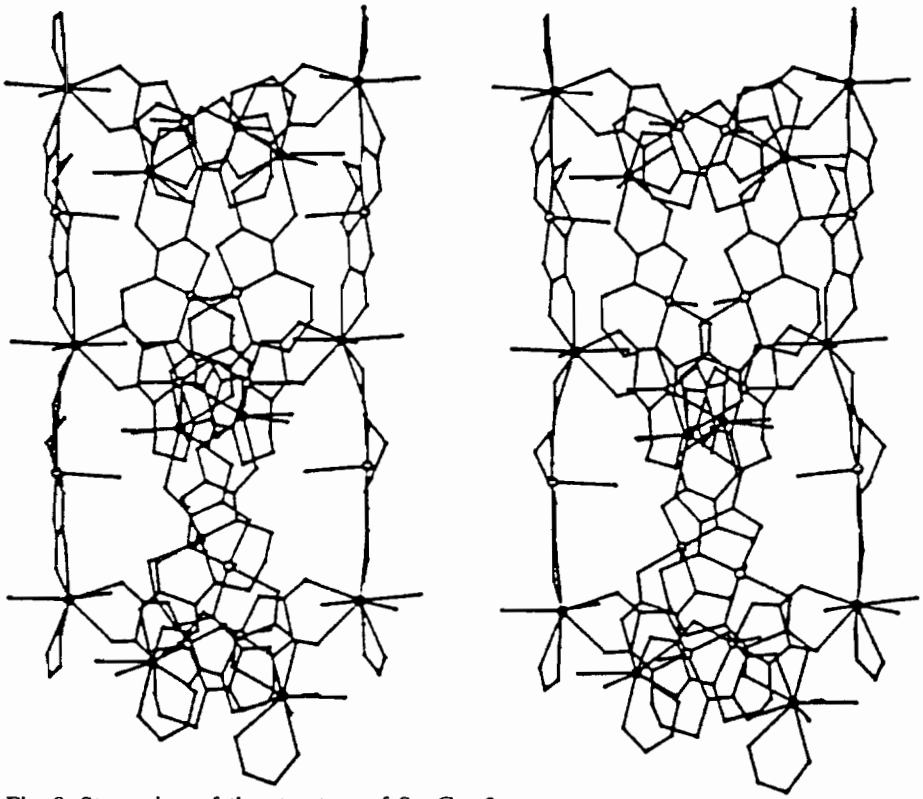

Fig. 8. Stereoview of the structure of $Sm_2Cu_3 \cdot 2$.

yttrium is not a rare earth). They have the electronic configuration of the noble gases [Kr] and [Xe], respectively. The question at hand is to know whether the copper(II) ions may interact through a diamagnetic rare earth in spite of the large Cu–M–Cu separation between two spin carriers, about 11.3 Å. If so, the temperature dependence of the magnetic susceptibility deviates from the Curie law expected for isolated copper(II) ions. Such a weak deviation is observed for $La_2Cu_3 \cdot 2$, as shown in Fig. 9. $\chi_M T$ is equal to 1.23 $cm^3\ K\ mol^{-1}$ above *c.* 10 K, which corresponds to what is expected for three non-coupled copper(II) ions. As the temperature is lowered, $\chi_M T$ slightly decreases, and seems to tend to zero as $T$ approaches the absolute

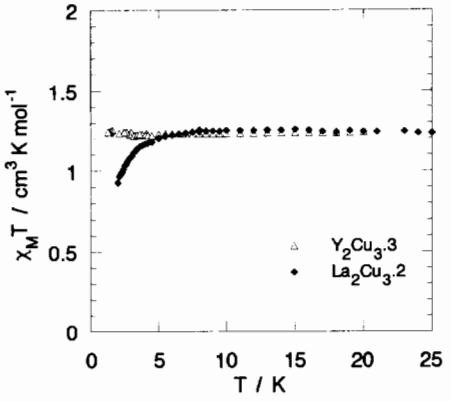


Fig. 9. $\chi_M T$ vs. $T$ plots for $La_2Cu_3$·**2** and $Y_2Cu_3$·**3**.

zero. Those magnetic data indicating an antiferromagnetic interaction can be resonably well fitted with a Curie–Weiss law $\chi_M = C/(T-\theta)$, $\theta$ being equal to $-0.2$ K. The magnitude of the interaction between two copper(II) ions through a La(III) ion may be estimated in the mean-field approximation. Indeed, $\theta$ is related to the $J$ exchange parameter ($H = -JS_A \cdot S_B$) through [35]

$$\theta = zJS(S+1)/3k$$

which leads to $J = -0.15$ cm$^{-1}$. The number of nearest neighbors $z$ is taken equal to 4; it is indeed assumed that the Cu(II)–Cu(II) interaction is entirely propagated through the rare earth ion, and not through space. A similar result is obtained with $La_2Cu_3Cu$·**1**.

In contrast, the magnetic susceptibility of $Y_2Cu_3$·**3** perfectly follows the Curie law down to 1.3 K (see Fig. 9). One sees, therefore, that La(III) transmits the interaction, but Y(III) does not. Two factors may account for this difference: (i) the ionic radius of La(III) is 0.18 Å smaller than that of Y(III), and consequently, the overlap integrals between rare earth and oxygen valence orbitals are larger in the former case, which is in line with the magnetic findings; (ii) the $5s^2\ 5p^6$ valence orbitals of La(III) are certainly more diffuse than the $4s^2\ 4p^6$ valence orbitals of Y(III), which again favors the rare earth–oxygen overlap integrals. In a certain sense, the difference between Y(III) and La(III) as far as the capability to propagate the interaction between magnetic centers is concerned is much the same as between oxygen and sulfur atoms. Owing to the diffuseness of the sulfur valence orbitals, sulfur-containing bridges transmit the interaction between magnetic centers much more efficiently than similar oxygen-containing bridges [36].

The interaction between two copper(II) ions is also propagated through the Eu(III) ion, the $^7F_0$ ground state of which is diamagnetic. When $T$ approaches the absolute zero, $\chi_M T$ for $Eu_2Cu_3$·**2** tends to zero and not to the value expected for three uncoupled copper(II) ions (*c.* 1.2 cm$^3$ K mol$^{-1}$).

*Compounds exhibiting a ferromagnetic-like behavior*

We implicitly mentioned in the introduction that the design of molecular-based magnets was one of the main challenges in the field of molecular materials [37]. When a new compound is synthesized, the first experimental information suggesting that it could behave as a magnet is the rapid increase of $\chi_M T$ upon cooling. This increase indicates that the ground state is more magnetic than the thermally populated excited states. If the compound consists of isolated clusters, $\chi_M T$ reaches a plateau in the low-temperature limit, with a value specifying the ground state spin. If, on the other hand, the compound has a one-dimensional character, $\chi_M T$ may reach very high values before declining owing to demagnetizing effect [38]. This rapid rise of $\chi_M T$ is due to the increase of the correlation length, i.e. of the length along which the local spins are ordered. If the compound, now, has some three-dimensional character, a magnetic transition may occur at a critical temperature $T_c$ with either a ferro- (or ferri-), or an antiferromagnetic state below $T_c$. In the former case, a spontaneous magnetization appears, and the magnetization versus magnetic field curve in general exhibits a hysteresis effect. In the latter case, both $\chi_M T$ and $\chi_M$ falls down. In one-dimensional compounds, the three-dimensional character may be due to weak interchain interactions.

To sum up, we can say that a rapid increase of $\chi_M T$ upon cooling is a necessary but not sufficient condition to have a magnet. This increase, however, does not provide any direct information on the nature of the interaction between nearest neighbor spin carriers. This interaction can be ferromagnetic; if so, all local spins tend to align parallel. It can be antiferromagnetic provided that there is no compensation of the local spins, which may happen in a bimetallic system when the $S_A$ and $S_B$ local spins are non-equivalent; the system is then a ferrimagnet. The increase of $\chi_M T$ can also arise from canted antiferromagnetic interactions with a small angle between nearest neighbor local spins which otherwise would align antiparallel [39]. Information concerning the ferro-, antiferro- or canted nature of the interaction may be deduced from the magnetization versus magnetic field curve, as will be discussed below.

Among all compounds mentioned in Table 1, only those containing Gd(III), Tb(III), Dy(III) and Er(III) exhibit an increase of $\chi_M T$ as $T$ is lowered. In this paper, we will consider in more detail the compounds $Gd_2Cu_3Cu$·**1** and $Dy_2Cu_3$·**3**.

The $\chi_M T$ versus $T$ plot for $Gd_2Cu_3Cu$·**1** is shown in Fig. 10. Down to *c.* 30 K, $\chi_M T$ is equal to 17.2 cm$^3$

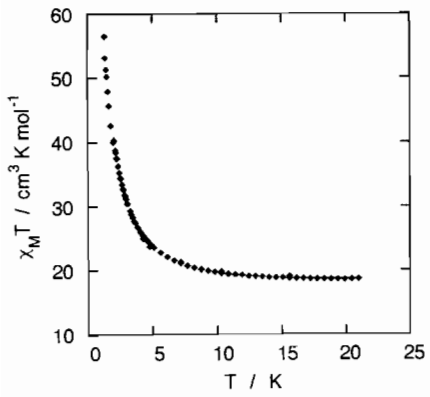


Fig. 10. $\chi_M T$ vs. $T$ plot for $Gd_2Cu_3Cu \cdot \mathbf{1}$.

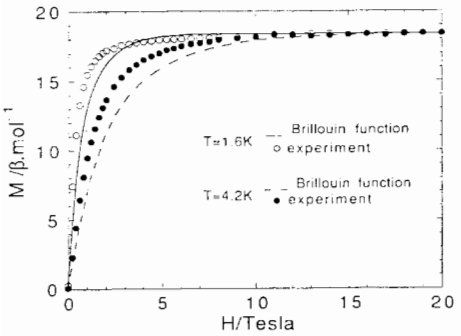


Fig. 11. Magnetization $M$ vs. magnetic field $H$ curves for $Gd_2Cu_3Cu \cdot \mathbf{1}$ at 1.6 and 4.2 K.

K mol$^{-1}$, which corresponds to what is expected for two Gd(III) and four Cu(II) non-interacting ions. As the temperature is lowered, $\chi_M T$ increases more and more rapidly and reaches 60 cm$^3$ K mol$^{-1}$ at 1.3 K, the lowest temperature we can reach with our magnetometers. Those data clearly indicate that the $S_{Gd}=7/2$ local spins tend to align parallel, but do not specify whether the $S_{Cu}=1/2$ local spins align along the same direction (ferromagnetic behavior) or along the opposite direction (ferrimagnetic behavior). The dependence of the molar magnetization $M$ as a function of the field $H$ was recorded at various temperatures below 5 K both in the low-field regime ($0 \leqslant H \leqslant 200$ G) and in the high-field regime ($0 \leqslant H \leqslant 20$ T). Up to 200 G, the magnetization is strictly linear versus the field, the slope being in perfect agreement with the magnetic susceptibility value measured independently. Those low-field measurements do not show any indication of spin decoupling, i.e. a change of sign of $d^2M/dH^2$. The experimental data in the high-field regime at 1.6 and 4.2 K are shown in Fig. 11 together with the theoretical curves for two Gd(III) and four Cu(II) non-coupled ions, i.e. Brillouin's functions. At both temperatures, the magnetization increases faster than expected for non-interacting ions. The saturation magnetization $M_S$ is equal to 18 N$\beta$, which exactly corresponds to the value anticipated when all local spins are aligned parallel. Those data unambiguously show that even in zero field all local spins tend to align parallel. The Gd(III)–Cu(II) interaction through the oxamato bridge is ferromagnetic. A more complete discussion concerning this problem can be found in ref. 33.

The $\chi_M T$ versus $T$ plot for $Dy_2Cu_3 \cdot \mathbf{3}$ is represented in Fig. 12. Down to 20 K, $\chi_M T$ is equal to 29.5 cm$^3$ K mol$^{-1}$. This value agrees with what is anticipated for two Dy(III) and three Cu(II) isolated ions. Indeed, Dy(III) has a $^6H_{15/2}$ ground state with a $g_{15/2}$ Zeeman factor equal to 4/3 so that the $\chi_M T$ value for a single Dy(III) ion is $N\beta^2 g_J^2 J(J+1)/3k = 14.14$ cm$^3$ K mol$^{-1}$, ignoring the temperature-independent paramagnetism. When $T$ is lowered below 20 K, $\chi_M T$ increases more and more rapidly, and reaches 90 cm$^3$ K mol$^{-1}$ at 1.8 K, which again indicates that the $J_{Dy}=15/2$ local momenta tend to align parallel. The magnetization versus magnetic field curve, measured at 2 K, does not show any sign of magnetic momentum decoupling, and is above the Brillouin curve for two Dy(III) and three Cu(II) uncoupled ions, which again suggests that all magnetic momenta tend to align parallel. The situation is however more complicated than for the Gd(III) compounds. As a matter of fact, owing to the orbital contribution, Dy(III) is strongly anisotropic. Magnetic anisotropy measurements are planned to obtain new insights on the physics of this material.

Gatteschi and co-workers reported on a $Dy(III)_2Cu(II)_2$ tetranuclear unit, and found that $\chi_M T$ for this compound slightly decreased upon cooling, which might be due to a mere crystal field effect splitting of the $^6H_{15/2}$ state into eight Kramers doublets. In other words, they did not observe any clear evidence of Dy(III)–Dy(III) or Dy(III)–Cu(II) interaction in their compound [21], which contrasts with our result concerning $Dy_2Cu_3 \cdot \mathbf{2}$.

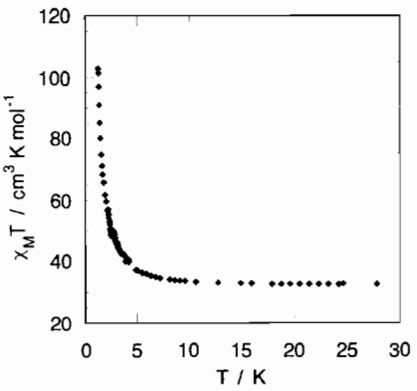


Fig. 12. $\chi_M T$ vs. $T$ plot for $Dy_2Cu_3 \cdot \mathbf{3}$.

## Conclusions

It is difficult to conclude a work which is still in progress. Actually, there are many more results to obtain and analyse than findings already obtained and interpreted. Using a unique copper(II) precursor, $[Cu(pba)]^{2-}$, three families of compounds have already been characterized. Nothing says that another family could not be discovered. We have begun exploring the reaction of rare earth ions with other precursors containing 3d metal ions.

The first rewarding facet of this area of research is the beauty and the originality of the crystal structures. In this paper, we have described a bimetallic ladder (structure **3**), then a two-dimensional arrangement of such ladders linked together by oxalato groups (structure **1**), and finally an unprecedented bimetallic tube with a four-fold symmetry, arising from the condensation of two ladders accompanied of a complete redistribution of the rungs (structure **2**). Furthermore, structure **1** contains $[Cu(H_2O)_5]^{2+}$ discrete units in the gaps between the two-dimensional layers. Preliminary results suggest that those $[Cu(H_2O)_5]^{2+}$ cations could be replaced by other charged species. More generally, all three structures possess rather broad channels in which are located non-coordinated water molecules. Maybe, some chemistry could be performed within those channels.

This short review paper at the best gives a flavour on the diversity of the magnetic properties of our compounds. The ferromagnetic nature of the Gd(III)–Cu(II) interaction had already been reported [19–22]. Our results confirm this phenomenon which is enhanced here since we are faced with one- or two-dimensional materials, and not a loose assembly of isolated molecular units. They also indicate that the same situation holds for Dy(III)–Cu(II) and probably also Tb(III)–Cu(II) and Er(III)–Cu(II). On the other hand, with the other non-diamagnetic rare earth M(III), the M(III)–Cu(II) interaction, if any, is rather antiferromagnetic in the sense where the magnetic momenta in zero field tend to align antiparallel. Concerning the Gd(III) containing compounds, a theoretical model has been established to calculate the magnetic properties of a Gd(III)Cu(II) ladder, the $S_{Gd}=7/2$ local spin of Gd(III) being treated as a classical spin. This model, however, is very complicated, and for sure outside the scope of this paper (and of this journal).

Concerning the interpretation of the magnetic properties of these materials, the strong orbital contribution to the ground state of most of the rare earth ions together with the subtlety of the crystal structures makes the problem difficult. Nevertheless, we expect to bring new insights soon, and to report on quite surprising results.

## Experimental

*Syntheses*

The sodium salt of the copper(II) precursor $Na_2[Cu(pba)]\cdot 6H_2O$ was synthesized as previously described [9, 40]. The compounds $M_2Cu_3Cu\cdot\mathbf{1}$ were obtained as blue plate-like single crystals by slow diffusion in a H-shaped tube at room temperature of equimolecular (0.025 mol $l^{-1}$) aqueous solutions of $Na_2[Cu(pba)]\cdot 6H_2O$ and $MCl_3\cdot 6H_2O$ within *c.* two months. M stands for La, Ce, Pr, Nd, Sm, Eu or Gd. The compounds $M_2Cu_3\cdot\mathbf{3}$ with M = Tb, Dy, Ho, Er, Tm, Yb and Y were obtained in exactly the same way as above. On the other hand, another method was used to prepare the compounds $M_2Cu_3\cdot\mathbf{2}$ with M = La, Ce, Pr, Nd, Sm, Eu or Gd. An aqueous solution of $Na_2[Cu(pba)]\cdot 6H_2O$ (0.05 mol $l^{-1}$) was added dropwise into an aqueous solution of rare earth(III) chloride (0.1 mol $l^{-1}$) under rigorous stirring. The solution was left stirring for a while, then filtered to eliminate the light blue precipitate. The dark blue solution was kept in a temperature-controlled bath at 70 °C. Large cube-like dark blue single crystals appeared within 48 h. The isomorphism of the compounds in each of the three families was checked by Debye–Scherrer photographs, and in several cases cell determinations.

*Crystallographic data collection and structure determination*

Blue prismatic crystals of $Dy_2Cu_3\cdot\mathbf{3}$, stable only in contact with their mother liquor, are particularly fragile. They have to be handled with extreme care. A single crystal was sealed in a thin-walled capillary with a small amount of the mother liquor, and mounted on an Enraf-Nonius CAD4-F diffractometer. Unit-cell dimensions and crystal orientation matrix were obtained from matrix least-squares refinements of setting angles of 25 reflections measured in the range $12.8<2\theta<23.6°$. Intensity data were checked for orientation (every 400 reflections) and for intensity (every hour of X-ray exposure time). The data were corrected for background, Lorentz–polarization, and absorption (DIFABS procedure [41]). The structure was solved by direct methods using MULTAN 11/82 [42] and difference Fourier techniques, and refined (on $F_o$s) by full matrix least-squares calculations, initially with isotropic, then with anisotropic thermal parameters for all non-hydrogen atoms, except oxygen atoms of water molecules which were refined isotropically. Hydrogen atoms of the pba ligand were included at idealized positions. Other pertinent crystallographic data are listed in Table 2. All calculations were performed on a DEC micro VAX II computer using the Enraf-Nonius SDP system of programs [43]. The positional parameters are listed in Table 3, selected bond lengths and angles in

TABLE 2. Experimental data for the X-ray diffraction study of $Dy_2Cu_3 \cdot 3$

| | |
|---|---|
| Molecular formula | $Dy_2Cu_3C_{21}N_6O_{41}H_{64}$ |
| Formula weight | 1572.5 |
| Crystal dimensions (mm) | $0.2 \times 0.1 \times 0.1$ |
| Temperature (K) | 293 |
| Crystal system | monoclinic |
| Space group | $P2_1/n$ |
| $a$ (Å) | 18.637(6) |
| $b$ (Å) | 16.025(2) |
| $c$ (Å) | 19.685(6) |
| $V$ (Å$^3$) | 5437(5) |
| $\beta$ (°) | 112.37(3) |
| $Z$ | 4 |
| $D_{calc}$ (g cm$^{-3}$) | 1.91 |
| $F(000)$ | 3116 |
| $\mu$ (cm$^{-1}$) | 40.1 |
| Radiation | Mo K$\alpha$ (graphite monochromated $\lambda = 0.71073$ Å) |
| Detector aperture (mm) | vertical slit 4, horizontal aperture $2.2 + 0.6\tan\theta$ |
| $hkl$ Range | $0 \leqslant h \leqslant 22$, $-1 \leqslant k \leqslant 19$, $-23 \leqslant l \leqslant 23$ |
| $\theta$ Range (°) | $1 \leqslant \theta \leqslant 25$ |
| Scan type | $\omega$–$2\theta$ |
| Scan speed (° min$^{-1}$) | variable |
| Scan width (°) | $1.00 + 0.35\tan\theta$ |
| Data collected | 11041 |
| Independent data | 9942 |
| Observed data ($I_{obs} \geqslant 3\sigma(I)$) | 3761 |
| Parameters refined | 578 |
| $R$[a] (%) | 4.8 |
| $R_w$[b] (%) | 6.9 |
| Goodness of fit | 1.314 |
| Final shift/error | 0.01 |
| Residual density (e Å$^{-3}$) | 1.25 (in the vicinity of a Dy atom) |

[a] $R = \Sigma \|K\|F_o\| - \|F_c\| / \Sigma K\|F_o\|$. [b] $R_w = [\Sigma w(K\|F_o\| - \|F_c\|)^2 / \Sigma w\|F_o\|^2]^{1/2}$; $w = 1/\sigma^2(\|F_o\|)$; $\sigma^2(F_o) = \sigma^2(I) + (0.08F_o^2)^2/4F_o^2$.

TABLE 3. Positional parameters and their e.s.d.s for $Dy_2Cu_3 \cdot 3$

| Atom | $x$ | $y$ | $z$ | $B$ (Å$^2$)[a] |
|---|---|---|---|---|
| Dy1 | 0.76492(4) | 0.14355(6) | 0.39991(4) | 2.37(2) |
| Dy2 | 1.12362(4) | 0.13780(5) | 0.04617(3) | 1.79(1) |
| Cu1 | 1.0072(1) | 0.2395(2) | 0.6620(1) | 4.62(7) |
| Cu2 | 1.3867(1) | 0.2504(1) | 0.2868(1) | 3.26(5) |
| Cu3 | 0.9253(1) | 0.1740(2) | 0.2056(1) | 3.28(5) |
| O101 | 0.6335(6) | 0.1199(8) | 0.3242(6) | 3.3(3) |
| O102 | 0.7045(7) | 0.2633(8) | 0.3355(6) | 4.5(3) |
| O103 | 0.7628(6) | 0.1123(8) | 0.2792(6) | 3.4(3) |
| O104 | 0.8760(6) | 0.1920(9) | 0.3856(6) | 3.8(3) |
| O105 | 0.8138(6) | 0.2493(8) | 0.4884(5) | 3.0(3) |
| O106 | 0.8687(7) | 0.0938(8) | 0.5039(6) | 3.6(3) |
| O107 | 0.6985(6) | 0.1318(8) | 0.4822(5) | 3.2(3) |
| O108 | 0.7547(8) | −0.0015(9) | 0.3937(7) | 5.2(4) |
| O201 | 1.0593(6) | 0.2564(8) | −0.0225(5) | 3.3(3) |
| O202 | 1.0422(6) | 0.1003(7) | −0.0739(5) | 2.7(3) |
| O203 | 0.9928(6) | 0.1090(8) | 0.0469(6) | 3.2(3) |
| O204 | 1.1068(6) | 0.1913(9) | 0.1481(5) | 3.7(3) |
| O205 | 1.2377(6) | 0.0986(8) | 0.1459(6) | 3.4(3) |
| O206 | 1.2117(5) | 0.2539(7) | 0.0913(5) | 2.1(2) |
| O207 | 1.2082(6) | 0.1288(8) | −0.0168(6) | 3.8(3) |
| O208 | 1.1233(6) | −0.0077(7) | 0.0503(6) | 2.8(3) |
| O11 | 0.9100(6) | 0.2866(8) | 0.5916(6) | 4.1(3) |
| O12 | 1.0325(7) | 0.3361(9) | 0.7281(6) | 4.7(4) |
| O13 | 1.076(1) | 0.301(1) | 0.5894(9) | 9.1(6) |
| O21 | 1.3377(6) | 0.1414(9) | 0.2455(5) | 3.8(3) |
| O22 | 1.4694(7) | 0.1989(8) | 0.3739(6) | 4.1(3) |
| O23 | 1.311(1) | 0.248(1) | 0.368(1) | 8.6(6) |
| O31 | 0.8270(6) | 0.1253(9) | 0.2045(6) | 4.2(3) |
| O32 | 0.9188(6) | 0.1189(7) | 0.1126(5) | 3.1(3) |
| O33 | 0.8526(8) | 0.287(1) | 0.1372(7) | 5.8(4) |
| N11 | 0.9733(9) | 0.144(1) | 0.6032(9) | 5.8(5) |
| N12 | 1.0988(9) | 0.191(1) | 0.7352(9) | 6.4(5) |
| N21 | 1.3101(7) | 0.2966(9) | 0.1974(6) | 2.5(3) |
| N22 | 1.4430(7) | 0.3512(8) | 0.3225(6) | 2.4(3) |
| N31 | 0.9409(8) | 0.203(1) | 0.3049(7) | 3.8(4) |
| N32 | 1.0285(8) | 0.206(1) | 0.2137(7) | 4.1(4) |
| C11 | 0.8751(8) | 0.237(1) | 0.5429(8) | 2.2(4) |
| C12 | 0.906(1) | 0.147(1) | 0.549(1) | 4.4(5) |
| C13 | 1.1391(9) | 0.243(1) | 0.7847(8) | 2.6(4) |
| C14 | 1.100(1) | 0.326(1) | 0.7795(8) | 3.5(4) |
| C15 | 1.014(1) | 0.051(2) | 0.617(2) | 11(1) |
| C16 | 1.090(2) | 0.061(2) | 0.665(2) | 17(1) |
| C17 | 1.133(2) | 0.105(2) | 0.726(2) | 15(1) |
| C21 | 1.2821(8) | 0.154(1) | 0.1863(7) | 2.4(4) |
| C22 | 1.2673(8) | 0.243(1) | 0.1553(7) | 2.0(4) |
| C23 | 1.4971(8) | 0.342(1) | 0.3858(7) | 2.0(4) |
| C24 | 1.5109(9) | 0.256(1) | 0.4158(7) | 2.6(4) |
| C25 | 1.306(1) | 0.389(1) | 0.1787(9) | 3.6(5) |

(continued)

TABLE 3. (*continued*)

| Atom | *x* | *y* | *z* | *B* (Å²)[a] |
|---|---|---|---|---|
| C26 | 1.343(2) | 0.442(2) | 0.239(2) | 12(1) |
| C27 | 1.420(1) | 0.435(1) | 0.290(1) | 5.3(6) |
| C31 | 0.818(1) | 0.136(1) | 0.2630(8) | 3.4(4) |
| C32 | 0.8844(9) | 0.183(1) | 0.3238(9) | 3.6(5) |
| C33 | 0.9809(8) | 0.133(1) | 0.1025(7) | 2.4(4) |
| C34 | 1.0442(9) | 0.182(1) | 0.1586(8) | 3.4(4) |
| C35 | 1.009(1) | 0.250(2) | 0.3566(9) | 5.2(6) |
| C36 | 1.067(1) | 0.256(2) | 0.332(1) | 15(1) |
| C37 | 1.086(1) | 0.250(2) | 0.2756(9) | 5.3(5) |
| OW1 | 0.2462(9) | 0.398(1) | 0.3762(8) | 7.2(4)* |
| OW2 | 0.830(1) | 0.383(1) | 0.3549(9) | 8.6(5)* |
| OW3 | 0.856(1) | 0.420(1) | 0.2243(9) | 8.5(5)* |
| OW4 | 0.138(1) | 0.468(1) | 0.2450(9) | 8.3(5)* |
| OW5 | 0.493(1) | 0.004(2) | 0.218(1) | 11.8(7)* |
| OW6 | 0.959(1) | 0.393(2) | 0.474(1) | 12.7(8)* |
| OW7 | 0.086(1) | 0.383(1) | 0.107(1) | 10.3(6)* |
| OW8 | 0.790(1) | 0.012(2) | 0.090(1) | 11.5(7)* |
| OW9 | 0.692(1) | 0.264(1) | 0.047(1) | 10.9(6)* |
| OW10 | 0.658(1) | 0.052(2) | 0.146(1) | 12.8(8)* |
| OW11 | 0.916(2) | 0.325(2) | 0.030(1) | 15.9(9)* |
| OW12 | 0.177(1) | 0.082(2) | 0.477(1) | 11.1(7)* |
| OW13 | 0.192(1) | 0.394(2) | 0.484(1) | 14.2(8)* |
| OW14 | 0.554(2) | 0.044(2) | 0.429(1) | 16(1)* |
| OW15 | 0.441(2) | 0.994(3) | 0.074(2) | 25(2)* |
| OW16 | 0.273(2) | 0.088(3) | 0.403(2) | 25(2)* |

[a]Starred atoms were isotropically refined. Anisotropically refined atoms are given in the form of the isotropic equivalent displacement parameter defined as: $(4/3)[a^2B(1,1)+b^2B(2,2)+c^2B(3,3)+ab(\cos\gamma)B(1,2)+ac(\cos\beta)B(1,3)+bc(\cos\alpha)B(2,3)]$.

TABLE 4. Selected bond distances (Å) for $Dy_2Cu_3\cdot 3$

| | | | | | |
|---|---|---|---|---|---|
| Dy1–O101 | 2.36(1) | Cu3–O31 | 1.98(1) | N21–C25 | 1.52(2) |
| Dy1–O102 | 2.34(1) | Cu3–O32 | 1.99(1) | N22–C23 | 1.28(2) |
| Dy1–O103 | 2.41(1) | Cu3–O33 | 2.35(2) | N22–C27 | 1.47(2) |
| Dy1–O104 | 2.33(1) | Cu3–N31 | 1.92(1) | O31–C31 | 1.24(2) |
| Dy1–O105 | 2.35(1) | Cu3–N32 | 1.94(1) | O32–C33 | 1.26(2) |
| Dy1–O106 | 2.35(1) | O101–C14 | 1.22(2) | N31–C32 | 1.28(2) |
| Dy1–O107 | 2.39(1) | O102–C13 | 1.25(2) | N31–C35 | 1.49(2) |
| Dy1–O108 | 2.33(1) | O103–C31 | 1.25(2) | N32–C34 | 1.29(2) |
| Dy2–O201 | 2.37(1) | O104–C32 | 1.29(2) | N32–C37 | 1.46(2) |
| Dy2–O202 | 2.35(1) | O105–C11 | 1.25(2) | C11–C12 | 1.53(3) |
| Dy2–O203 | 2.48(1) | O106–C12 | 1.24(2) | C13–C14 | 1.51(3) |
| Dy2–O204 | 2.31(1) | O201–C24 | 1.22(2) | C15–C16 | 1.38(3) |
| Dy2–O205 | 2.36(1) | O202–C23 | 1.29(2) | C16–C17 | 1.36(4) |
| Dy2–O206 | 2.42(1) | O203–C33 | 1.26(2) | C21–C22 | 1.53(2) |
| Dy2–O207 | 2.35(1) | O204–C34 | 1.27(2) | C23–C24 | 1.48(2) |
| Dy2–O208 | 2.33(1) | O205–C21 | 1.27(2) | C25–C26 | 1.41(3) |
| Cu1–O11 | 1.96(1) | O206–C22 | 1.30(2) | C26–C27 | 1.40(3) |
| Cu1–O12 | 1.96(1) | O11–C11 | 1.23(2) | C31–C32 | 1.55(2) |
| Cu1–O13 | 2.45(2) | O12–C14 | 1.29(2) | C33–C34 | 1.50(2) |
| Cu1–N11 | 1.88(2) | N11–C15 | 1.64(4) | C35–C36 | 1.36(3) |
| Cu1–N12 | 1.93(1) | N11–C12 | 1.31(2) | C36–C37 | 1.29(3) |
| Cu2–O21 | 1.99(1) | N12–C17 | 1.55(3) | | |
| Cu2–O22 | 2.00(1) | N12–C13 | 1.29(2) | | |
| Cu2–O23 | 2.51(2) | O21–C21 | 1.25(2) | | |
| Cu2–N21 | 1.94(1) | O22–C24 | 1.28(2) | | |
| Cu2–N22 | 1.91(1) | N21–C22 | 1.24(2) | | |

Numbers in parentheses are e.s.d.s in the least significant digits.

Tables 4 and 5, respectively, and intermetallic distances in Table 6. See also 'Supplementary material'.

*Magnetic measurements*

These were carried out with three apparatus, namely a Faraday type magnetometer working in the 4.2–300 K temperature range, an a.c. inductance bridge magnetometer working in zero field in the 1.3–10 K temperature range, and finally a SQUID magnetometer working both in the low-field (a few Gauss) and the high-field (up to 8 Tesla) regime down to 1.8 K. Special care was taken to avoid the orientation of the crystallites along the field for the compounds containing strongly anisotropic rare earths.

*Supplementary material*

Positional and isotropic thermal parameters of hydrogen atoms (Table S1), anisotropic thermal parameters (Table S2), and listing of calculated and observed structure factors (21 pages) may be obtained on request from the authors.

TABLE 5. Bond angles (°) for $Dy_2Cu_3\cdot 3$

| | | | |
|---|---|---|---|
| O101–Dy1–O102 | 67.7(4) | O201–Dy2–O202 | 68.9(4) |
| O101–Dy1–O103 | 73.8(4) | O201–Dy2–O203 | 82.4(4) |
| O101–Dy1–O104 | 137.2(4) | O201–Dy2–O204 | 89.5(5) |
| O101–Dy1–O105 | 126.8(4) | O201–Dy2–O205 | 141.7(4) |
| O101–Dy1–O106 | 143.5(4) | O201–Dy2–O206 | 73.6(4) |
| O101–Dy1–O107 | 74.7(4) | O201–Dy2–O207 | 92.5(4) |
| O101–Dy1–O108 | 76.3(4) | O201–Dy2–O208 | 144.3(3) |
| O102–Dy1–O103 | 79.2(4) | O202–Dy2–O203 | 72.5(4) |
| O102–Dy1–O104 | 85.8(5) | O202–Dy2–O204 | 136.0(4) |
| O102–Dy1–O105 | 77.4(4) | O202–Dy2–O205 | 143.1(4) |
| O102–Dy1–O106 | 144.6(4) | O202–Dy2–O206 | 130.9(4) |
| O102–Dy1–O107 | 99.5(5) | O202–Dy2–O207 | 76.1(4) |
| O102–Dy1–O108 | 140.9(4) | O202–Dy2–O208 | 76.7(4) |
| O103–Dy1–O104 | 68.4(4) | O203–Dy2–O204 | 66.8(4) |
| O103–Dy1–O105 | 137.4(4) | O203–Dy2–O205 | 121.3(4) |
| O103–Dy1–O106 | 119.1(4) | O203–Dy2–O206 | 132.2(4) |
| O103–Dy1–O107 | 146.3(4) | O203–Dy2–O207 | 147.9(4) |
| O103–Dy1–O108 | 76.7(5) | O203–Dy2–O208 | 78.4(4) |
| O104–Dy1–O105 | 74.8(4) | O204–Dy2–O205 | 75.7(4) |
| O104–Dy1–O106 | 75.2(5) | O204–Dy2–O206 | 72.1(4) |
| O104–Dy1–O107 | 145.3(4) | O204–Dy2–O207 | 145.1(4) |
| O104–Dy1–O108 | 112.6(5) | O204–Dy2–O208 | 109.7(5) |
| O105–Dy1–O106 | 69.0(4) | O205–Dy2–O206 | 68.2(4) |
| O105–Dy1–O107 | 73.1(4) | O205–Dy2–O207 | 81.4(4) |
| O105–Dy1–O108 | 139.3(4) | O205–Dy2–O208 | 73.7(4) |
| O106–Dy1–O107 | 81.3(4) | O206–Dy2–O207 | 75.1(4) |
| O106–Dy1–O108 | 74.4(4) | O206–Dy2–O208 | 140.1(3) |
| O107–Dy1–O108 | 84.5(5) | O207–Dy2–O208 | 88.2(4) |
| O11–Cu1–O12 | 95.0(5) | O21–Cu2–O22 | 94.1(5) |
| O11–Cu1–O13 | 88.9(6) | O21–Cu2–O23 | 88.0(6) |
| O11–Cu1–N11 | 83.0(6) | O21–Cu2–N21 | 84.3(5) |
| O11–Cu1–N12 | 176.0(8) | O21–Cu2–N22 | 173.3(6) |

(*continued*)

TABLE 5. (*continued*)

| | | | |
|---|---|---|---|
| O12–Cu1–O13 | 91.4(7) | O22–Cu2–O23 | 83.1(6) |
| O12–Cu1–N11 | 172.7(8) | O22–Cu2–N21 | 175.6(6) |
| O12–Cu1–N12 | 84.4(6) | O22–Cu2–N22 | 84.1(5) |
| O13–Cu1–N11 | 95.5(8) | O23–Cu2–N21 | 100.9(6) |
| O13–Cu1–N12 | 95.1(8) | O23–Cu2–N22 | 98.1(6) |
| N11–Cu1–N12 | 97.1(7) | N21–Cu2–N22 | 97.0(5) |
| O31–Cu3–O32 | 94.8(5) | O32–Cu3–O33 | 89.7(5) |
| O31–Cu3–O33 | 88.2(6) | O32–Cu3–N31 | 166.9(6) |
| O31–Cu3–N31 | 83.5(6) | O32–Cu3–N32 | 84.6(5) |
| O31–Cu3–N32 | 171.5(7) | O33–Cu3–N31 | 103.2(6) |
| N31–Cu3–N32 | 95.2(6) | O33–Cu3–N32 | 100.2(7) |
| Dy1–O101–C14 | 118.0(1) | Dy2–O201–C24 | 117.0(1) |
| Dy1–O102–C13 | 119.0(1) | Dy2–O202–C23 | 117.0(9) |
| Dy1–O103–C31 | 119.0(1) | Dy2–O203–C33 | 117.0(1) |
| Dy1–O104–C32 | 121.0(1) | Dy2–O204–C34 | 122.3(9) |
| Dy1–O105–C11 | 119.0(1) | Dy2–O205–C21 | 120.0(1) |
| Dy1–O106–C12 | 116.0(1) | Dy2–O206–C22 | 116.0(1) |
| Cu1–O11–C11 | 112.0(1) | Cu3–N31–C35 | 125.0(1) |
| Cu1–O12–C14 | 110.0(1) | C32–N31–C35 | 120.0(2) |
| Cu2–O21–C21 | 109.0(1) | Cu3–N32–C34 | 113.0(1) |
| Cu2–O22–C24 | 110.0(1) | Cu3–N32–C37 | 126.0(1) |
| Cu3–O31–C31 | 113.0(1) | C34–N32–C37 | 122.0(2) |
| Cu3–O32–C33 | 109.1(9) | O105–C11–O11 | 127.0(2) |
| Cu1–N11–C12 | 117.0(2) | O105–C11–C12 | 114.0(2) |
| Cu1–N11–C15 | 128.0(1) | O11–C11–C12 | 118.0(1) |
| C12–N11–C15 | 115.0(2) | O106–C12–N11 | 131.0(2) |
| Cu1–N12–C13 | 113.0(1) | O106–C12–C11 | 120.0(2) |
| Cu1–N12–C17 | 124.0(1) | N11–C12–C11 | 109.0(2) |
| C13–N12–C17 | 121.0(2) | O102–C13–N12 | 132.0(2) |
| Cu2–N21–C22 | 114.0(1) | O102–C13–C14 | 115.0(2) |
| Cu2–N21–C25 | 122.9(9) | N12–C13–C14 | 113.0(1) |
| C22–N21–C25 | 123.0(1) | O101–C14–C13 | 118.0(2) |
| Cu2–N22–C23 | 113.0(1) | O101–C14–O12 | 124.0(2) |
| Cu2–N22–C27 | 125.7(9) | O12–C14–C13 | 118.0(2) |
| C23–N22–C27 | 121.0(1) | N11–C15–C16 | 107.0(2) |
| Cu3–N31–C32 | 114.0(1) | C15–C16–C17 | 141.0(4) |
| N12–C17–C16 | 116.0(2) | O103–C31–O31 | 128.0(2) |
| O205–C21–O21 | 125.0(2) | O103–C31–C32 | 116.0(1) |
| O205–C21–C22 | 115.0(1) | O31–C31–C32 | 116.0(2) |
| O21–C21–C22 | 119.0(1) | O104–C32–N31 | 131.0(2) |
| O206–C22–N21 | 129.0(2) | O104–C32–C31 | 116.0(2) |
| O206–C22–C21 | 118.0(1) | N31–C32–C31 | 113.0(2) |
| N21–C22–C21 | 114.0(1) | O203–C33–O32 | 124.0(1) |
| O202–C23–N22 | 127.0(2) | O203–C33–C34 | 117.0(1) |
| O202–C23–C24 | 116.0(1) | O32–C33–C34 | 119.0(1) |
| N22–C23–C24 | 116.0(1) | O204–C34–N32 | 128.0(1) |
| O201–C24–C23 | 120.0(1) | O204–C34–C33 | 117.0(1) |
| O201–C24–O22 | 124.0(2) | N32–C34–C33 | 114.0(2) |
| O22–C24–C23 | 116.0(1) | N31–C35–C36 | 112.0(2) |
| N21–C25–C26 | 115.0(2) | C35–C36–C37 | 145.0(2) |
| C25–C26–C27 | 127.0(3) | N32–C37–C36 | 114.0(2) |
| N22–C27–C26 | 115.0(2) | | |

(*continued*)

Numbers in parentheses are e.s.d.s in the least significant digits

TABLE 6. Selected intermetallic distances

| | Symmetry | Distance | | Symmetry | Distance |
|---|---|---|---|---|---|
| Shortest intramolecular intermetallic distances | | | | | |
| Dy1–Dy1 | $(x-\frac{1}{2}, \frac{1}{2}-y, z-\frac{1}{2})$ | 11.2007(6) | Dy1–Dy1 | $(x+\frac{1}{2}, \frac{1}{2}-y, z+\frac{1}{2})$ | 11.2007(6) |
| Dy1–Dy2 | $(x, y, z)$ | 11.3390(10) | Dy1–Cu1 | $(x, y, z)$ | 5.6228(22) |
| Dy1–Cu1 | $(x-\frac{1}{2}, \frac{1}{2}-y, z-\frac{1}{2})$ | 5.6013(22) | Dy1–Cu2 | $(x, y, z)$ | 12.7141(27) |
| Dy1–Cu2 | $(x-\frac{1}{2}, \frac{1}{2}-y, z-\frac{1}{2})$ | 13.2129(25) | Dy1–Cu3 | $(x, y, z)$ | 5.7012(23) |
| Dy2–Dy2 | $(x-\frac{1}{2}, \frac{1}{2}-y, z-\frac{1}{2})$ | 11.2583(6) | Dy2–Dy2 | $(x+\frac{1}{2}, \frac{1}{2}-y, z+\frac{1}{2})$ | 11.2583(6) |
| Dy2–Cu1 | $(x-\frac{1}{2}, \frac{1}{2}-y, z-\frac{1}{2})$ | 12.6810(30) | Dy2–Cu1 | $(x, y, z)$ | 13.2033(29) |
| Dy2–Cu2 | $(x-\frac{1}{2}, \frac{1}{2}-y, z-\frac{1}{2})$ | 5.6522(20) | Dy2–Cu2 | $(x, y, z)$ | 5.6587(20) |
| Dy2–Cu3 | $(x, y, z)$ | 5.7143(23) | Cu1–Cu1 | $(x-\frac{1}{2}, \frac{1}{2}-y, z-\frac{1}{2})$ | 10.6739(2) |
| Cu1–Cu1 | $(x+\frac{1}{2}, \frac{1}{2}-y, z+\frac{1}{2})$ | 10.6739(2) | Cu1–Cu2 | $(x, y, z)$ | 12.0121(36) |
| Cu1–Cu3 | $(x, y, z)$ | 8.5860(34) | Cu1–Cu3 | $(x+\frac{1}{2}, \frac{1}{2}-y, z+\frac{1}{2})$ | 7.6296(35) |
| Cu2–Cu2 | $(x+\frac{1}{2}, \frac{1}{2}-y, z+\frac{1}{2})$ | 10.6686(0) | Cu2–Cu2 | $(x-\frac{1}{2}, \frac{1}{2}-y, z-\frac{1}{2})$ | 10.6686(0) |
| Cu2–Cu3 | $(x+\frac{1}{2}, \frac{1}{2}-y, z+\frac{1}{2})$ | 8.2123(32) | Cu2–Cu3 | $(x, y, z)$ | 8.0899(31) |
| Cu3–Cu3 | $(x+\frac{1}{2}, \frac{1}{2}-y, z+\frac{1}{2})$ | 10.9434(11) | Cu3–Cu3 | $(x-\frac{1}{2}, \frac{1}{2}-y, z-\frac{1}{2})$ | 10.9434(11) |
| Shortest intermolecular intermetallic distances | | | | | |
| Dy1–Dy1 | $(2-x, -y, 1-z)$ | 9.3331(16) | Dy1–Dy | $(-x+\frac{1}{2}, -\frac{3}{2}+y, -z-\frac{1}{2})$ | 9.8409(8) |
| Dy1–Dy1 | $(\frac{1}{2}-x, y-\frac{1}{2}, -z-\frac{1}{2})$ | 9.8409(8) | Dy1–Dy2 | $(x-\frac{1}{2}, \frac{1}{2}-y, z+\frac{1}{2})$ | 5.7675(11) |
| Dy1–Cu1 | $(2-x, -y, 1-z)$ | 7.8169(29) | Dy1–Cu2 | $(2-x, -y, 1-z)$ | 6.7514(24) |
| Dy1–Cu2 | $(x-\frac{1}{2}, \frac{1}{2}-y, z+\frac{1}{2})$ | 7.2717(22) | Dy1–Cu3 | $(2-x, -y, 1-z)$ | 9.2401(25) |
| Dy1–Cu3 | $(-x+\frac{1}{2}, -\frac{3}{2}+y, -z-\frac{1}{2})$ | 8.2394(28) | Dy1–Cu3 | $(\frac{1}{2}-x, y-\frac{1}{2}, -z-\frac{1}{2})$ | 9.1380(26) |
| Dy2–Cu1 | $(2-x, -y, 1-z)$ | 9.2827(31) | Dy2–Cu1 | $(x+\frac{1}{2}, \frac{1}{2}-y, z-\frac{1}{2})$ | 6.9076(25) |
| Dy2–Cu1 | $(x, y, z-1)$ | 7.2166(26) | Dy2–Cu2 | $(\frac{3}{2}-x, y-\frac{3}{2}, -z-\frac{1}{2})$ | 7.0623(25) |
| Dy2–Cu3 | $(-x+2, -y, -z)$ | 6.8489(23) | Cu1–Cu1 | $(2-x, -y, 1-z)$ | 9.9162(53) |
| Cu1–Cu1 | $(-x+2, -y+1, -z+1)$ | 10.4471(58) | Cu1–Cu2 | $(x-\frac{1}{2}, \frac{1}{2}-y, z+\frac{1}{2})$ | 3.9124(36) |
| Cu1–Cu3 | $(2-x, -y, 1-z)$ | 7.0552(38) | Cu1–Cu3 | $(-x+2, -y+1, -z+1)$ | 9.7074(36) |
| Cu2–Cu2 | $(-x+\frac{3}{2}, -\frac{3}{2}+y, -z-\frac{1}{2})$ | 9.3057(24) | Cu2–Cu2 | $(-x+\frac{3}{2}, y-\frac{1}{2}, -z-\frac{1}{2})$ | 9.3057(24) |
| Cu2–Cu3 | $(-x+\frac{3}{2}, -\frac{3}{2}+y, -z-\frac{1}{2})$ | 9.8592(34) | Cu2–Cu3 | $(-x+\frac{3}{2}, y-\frac{1}{2}, -z-\frac{1}{2})$ | 7.6130(34) |
| Cu3–Cu3 | $(-x+\frac{1}{2}, -\frac{3}{2}+y, -z-\frac{1}{2})$ | 10.8906(30) | Cu3–Cu3 | $(\frac{1}{2}-x, y-\frac{1}{2}, -z-\frac{1}{2})$ | 10.8906(30) |
| Cu3–Cu3 | $(-x+2, -y, -z)$ | 11.0217(43) | Dy2–Dy2 | $(-x+2, -y, -z)$ | 6.1352(16) |

## References


1 O. Kahn, *Struct. Bonding (Berlin), 68* (1987) 89.
2 O Kahn, J.Galy, Y. Journaux, J. Jaud and I. Morgenstern-Badarau, *J. Am. Chem. Soc., 104* (1982) 2165.
3 Y. Journaux, O. Kahn, J. Zarembowitch, J. Galy and J. Jaud, *J. Am. Chem. Soc., 105* (1983) 7585.
4 Y. Pei. Y. Journaux and O. Kahn, *Inorg. Chem., 28* (1989) 100.
5 Y. Pei, Y. Journaux and O. Kahn, *Inorg. Chem., 27* (1988) 399.
6 A. Caneschi, D. Gatteschi, J. Laugier, P. Rey, R. Sessoli and C. Zanchini, *J. Am. Chem. Soc., 110* (1988) 2795.
7 M. Verdaguer, M.Julve, A. Michalowicz and O. Kahn, *Inorg. Chem., 22* (1983) 2624.
8 A. Gleizes and M. Verdaguer, *J. Am. Chem. Soc., 106* (1984) 3727.
9 Y. Pei, J. Sletten and O. Kahn, *J. Am. Chem. Soc., 108* (1986) 3143.
10 Y. Pei, M. Verdaguer, O. Kahn, J. Sletten and J. P. Renard, *J. Am. Chem. Soc., 108* (1986) 7428.
11 K. Nakatani, J. Y. Carriat, Y. Journaux, O. Kahn, F. Lloret, J. P. Renard; Y. Pei, J. Sletten and M. Verdaguer, *J. Am. Chem. Soc., 111* (1989) 5739.
12 K. Nakatani, P. Bergerat, E. Codjovi, C. Mathonière and O. Kahn, *Inorg. Chem., 30* (1991) 3978.
13 D. Beltran, E. Escriva and M. Drillon, *J. Chem. Soc., Faraday Trans. 2, 78* (1982) 1773.
14 M. Drillon, E. Coronada, D. Beltran and R. Georges, *J. Appl. Phys., 57* (1984) 3353.
15 M. Drillon, E. Coronado, D. Beltran, J. Curely, P. R. Nugteren, L. J. de Jongh and J. L. Genicon, *J. Magn. Magn. Mater., 54–57* (1986) 1507.
16 M. Drillon, E. Coronado, R. Gorges, J. C. Ganguzzo and J. Curely, *Phys. Rev. B, 40* (1989) 10992.
17 A. Caneschi, D. Gatteschi, J. P. Renard, P. Rey and R. Sessoli, *Inorg. Chem., 28* (1989) 1976.
18 A.Caneschi, D. Gatteschi, R. Sessoli and P. Rey, *Acc. Chem. Res., 22* (1989) 392.
19 A. Bencini, C. Benelli, A. Caneschi, R. L. Carlin, A. Dei and D. Gatteschi, *J. Am. Chem. Soc., 107* (1985) 8128.
20 A. Bencini, C. Benelli, A. Caneschi, A. Dei and D. Gatteschi, *Inorg. Chem., 25* (1986) 572.
21 C. Benelli, A. Caneschi, D. Gatteschi, O. Guillou and L. Pardi, *Inorg. Chem., 29* (1990) 1751.
22 N. Matsumoto, M. Sakamoto, H. Tamaki, H. Okawa and S. Kida, *Chem. Lett.,* (1989) 853.
23 W. Ollendorff and F. Weigel, *Inorg. Nucl. Chem. Lett., 5* (1969) 263.
24 A. Michaelides, S. Skoulika and A. Aubry, *Mater. Res. Bull., 23* (1988) 579.
25 J. C. Trombe, A. Gleizes and J. Galy, *C.R. Acad. Sci. Paris, Série II, 294* (1982) 1369; *Inorg. Chim. Acta, 87* (1984) 129.
26 J. F. Petit, J. C. Trombe, A. Gleizes and J. Galy, *C. R. Acad. Sci. Paris, Série II, 304* (1987) 1117.
27 A. Gleizes, F. Maury and J. Galy, *Nouv. J. Chim., 8* (1984) 521.
28 C. Frasse, J. C. Trombe, A. Gleizes and J. Galy, *C. R. Acad. Sci., Paris, Série II, 300* (1985) 403.
29 J. C. Trombe, C. Frasse and A. Gleizes, *C. R. Acad. Sci. Paris, Série II, 301* (1985) 483.
30 D. M. L. Goodgame, D. J. Williams and R. E. P. Winpenny, *Polyhedron, 12* (1989) 1531.
31 S. Wang, *Inorg. Chem., 30* (1991) 2252.
32 J. Blake, P. E. Y. Milne, P. Thornton and R. E. P. Winpenny, *Angew. Chem., Int. Ed. Engl., 30* (1991) 1139.
33 O. Guillou, P. Bergerat, O. Kahn, E. Bakalbassis, K. Boubekeur, P. Batail and M. Guillot, *Inorg. Chem., 31* (1991) 110.
34 O. Guillou, R. Oushoorn, O. Kahn, K. Boubekeur and P. Batail, *Angew. Chem., Int. Ed. Engl.,* in press.
35 C. J. O'Connor, *Prog. Inorg. Chem., 29* (1982) 203.
36 O. Kahn, *Angew. Chem., Int. Ed. Engl., 24* (1985) 834.
37 D. Gatteschi, O. Kahn, J. S. Miller and F. Palacio (eds.), *Magnetic Molecular Materials,* NATO ASI Series E, Vol. 198, Kluwer, Dordrecht, 1991.
38 F. Palacio, in D. Gatteschi, O. Kahn, J. S. Miller and F. Palacio (eds.), *Magnetic Molecular Materials,* NATO ASI Series E, Vol. 198, Kluwer, Dordrecht, 1991, p.1.
39 O. Kahn, in D. Gatteschi, O. Kahn, J. S. Miller and F. Palacio (eds.), *Magnetic Molecular Materials,* NATO ASI Series E, Vol. 198, Kluwer, Dordrecht, 1991, p 35.
40 K. Nonoyama, H. Ojima and M. Nonoyama, *Inorg. Chim. Acta, 20* (1976) 127.
41 D. Suart and M. Walker, *Acta Crystallogr., Sect. A, 39* (1983) 159.
42 P. Main, S. J. Fiske, S. E. Hull, L. Lessinger, G. Germain, J. P. Declercq and M. M. Woolfson, *MULTAN 11/82,* a system of computer programs for the automatic solution of crystal structures from X-ray diffraction data, University of York, UK and University of Louvain, Belgium, 1982.
43 B. A. Frenz, *Enraf-Nonius Structure Determination Package, SDP Users Guide,* Version Jan. 6, 1983, Enraf-Nonius, Delft, Netherlands, 1983.